ACS Energy LETTERS

Cite This: ACS Energy Lett. 2019, 4, 411−416

http://pubs.acs.org/journal/aelccp

LETTER

Regulating Anions in the Solvation Sheath of Lithium Ions for Stable Lithium Metal Batteries

Xue-Qiang Zhang,[†] Xiang Chen,[†] Li-Peng Hou,[†] Bo-Quan Li,[†] Xin-Bing Cheng,[†] Jia-Qi Huang,[‡] and Qiang Zhang*,[†]

[†]Beijing Key Laboratory of Green Chemical Reaction Engineering and Technology, Department of Chemical Engineering, Tsinghua University, Beijing 100084, China

[‡]Advanced Research Institute for Multidisciplinary Science, Beijing Institute of Technology, Beijing 100081, China

Supporting Information

ABSTRACT: Safe lithium (Li) metal batteries have been plagued by dendrite growth due to a heterogeneous solid electrolyte interphases (SEI) on the Li metal anode. Modulating the solvation sheath of Li ions enhances the uniformity and stability of SEI significantly. However, anion regulation in the solvation sheath for constructing stable SEI is rarely touched. Herein, the solvation structure of original bis(fluorosulfonyl)imide (FSI^-) anions in the solvation sheath is altered by introduction of other anions, promoting the complete decomposition of FSI^- and forming a stable SEI on the Li metal anode. Moreover, both the oxidation stability window of the electrolyte and current collector protection were enhanced. Furthermore, the components and structure of the solvation sheath were disclosed by combining ^{17}O nuclear magnetic resonance and molecular dynamics simulations. This work provides fresh insight into the interrelation among various anions on regulating the solvation sheath of Li ions and demonstrates guidance in rationally designing electrolytes for stable and safe Li metal batteries.

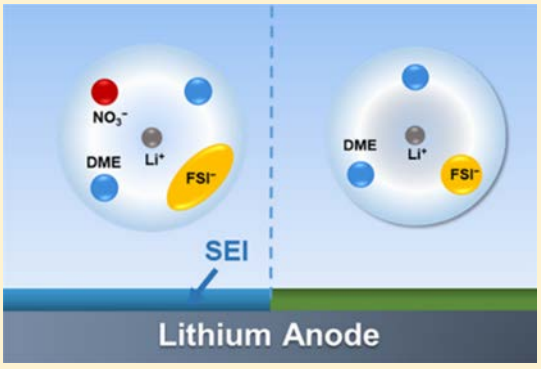

Lithium (Li) metal is the most attractive anode candidate for high-energy-density batteries for its high theoretical specific capacity (3860 mAh g^{-1}) and low reduction potential (−3.04 V vs standard hydrogen electrode).[1] Li metal batteries are being revived due to the increasing demand from portable electronics and electric vehicles. However, practical Li metal batteries are hindered by safety risks owing to dendrite growth.[2−4] In principle, dendrite growth is induced by nonuniform Li plating through heterogeneous solid electrolyte interphases (SEI).[5−7] Therefore, understanding the SEI formation process and constructing stable and uniform SEI are vital for promoting practical Li metal batteries.

The ingredients of SEI are derived from the reduction products between the electrolyte and highly reactive Li metal.[8−10] Concretely, Li ions are solvated by solvents and anions, forming a solvation sheath in the electrolyte.[11] Hence, the preferential decomposition products from solvents and anions in the solvation sheath compose the main components of SEI.[12] Regulating the components and structure of the solvation sheath of Li ions provides an effective route to construct uniform and stable SEI.

Many strategies have been devoted to regulating the solvation sheath of Li ions from solvation components and structure. In terms of components, the types of solvents,[13−17] anions,[18,19] and even additives[20,21] in the solvation sheath have significant effects on the uniformity of SEI. For instance, fluorinated carbonates or ethers can improve the uniformity of SEI by increasing the content of F-rich species.[22,23] There is preferential conscription of solvents in the structure of the solvation sheath of Li ions. Cyclic carbonate solvents are solvated more easily in comparison to linear carbonate solvents, forming the inner solvation sheath.[24] The solvation structure also changes evidently with the increased concentration of Li salts.[25−27] On one hand, the anodic or cathodic stability window of the electrolyte can be enlarged with decreasing free solvents, such as the concept of aqueous Li ion batteries with ultrahigh concentrated electrolyte.[28,29] On the other hand, partial anions can be recruited into the solvation sheath as the free solvents decrease, resulting in the

Received: December 6, 2018
Accepted: January 7, 2019
Published: January 7, 2019

DOI: 10.1021/acsenergylett.8b02376
ACS Energy Lett. 2019, 4, 411−416

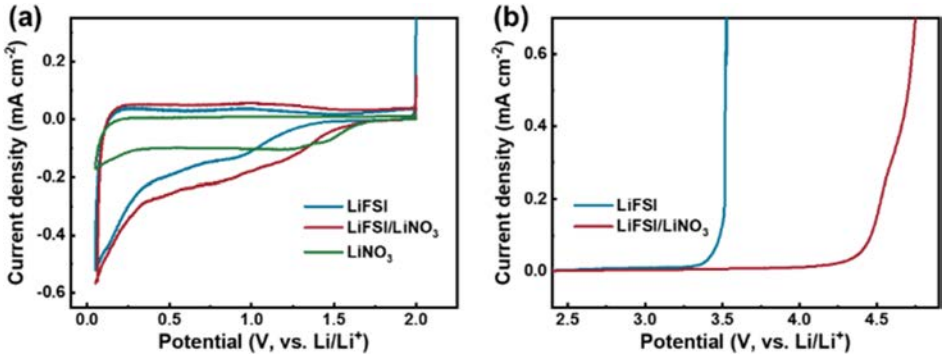

Figure 1. Cyclic voltammogram curves of (a) reduction behaviors and linear sweep voltammetry curves of (b) oxidation behaviors of electrolytes using a carbon-coated current collector as the working electrode and Li as the counter and reference electrode with a scan rate of 0.5 mV s^{-1}. The green line is 0.20 M $LiNO_3$ in DME. LiFSI (2.0 M) in DME (LiFSI electrolyte) is the control electrolyte.

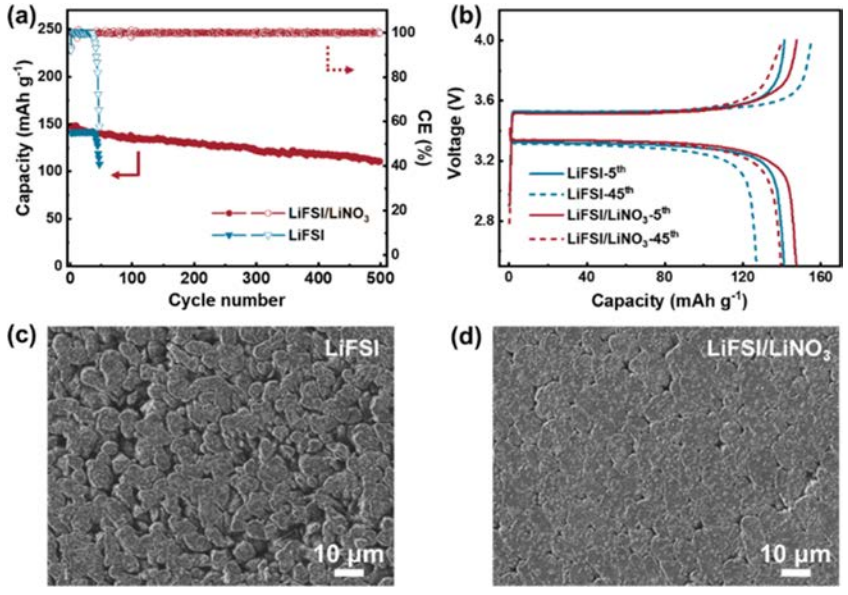

Figure 2. Electrochemical performance of Li|$LiFePO_4$ batteries with LiFSI or LiFSI/$LiNO_3$ electrolyte. (a) Cycle life and CE of Li|$LiFePO_4$ batteries at 1.0 C. (b) Voltage−capacity curves of Li|$LiFePO_4$ batteries. Deposition morphology of the Li anode with (c) LiFSI and (d) LiFSI/$LiNO_3$ electrolyte with a capacity of 2.0 mAh cm^{-2} after 10 cycles in Li|Li cells.

decomposed anions as ingredients of SEI.[30] Although the anions are indispensable, the anions in the solvation sheath and regulating anions for constructing stable SEI are rarely involved. If the interactions among different types of anions in the solvation sheath can be well understood, new adventures will be opened for regulating the solvation sheath of Li ions for stable and safe Li metal batteries.

In previous reports, $LiNO_3$ is proved to be effective in improving the performance of Li metal batteries.[31−33] However, the effects of $LiNO_3$ are mainly obtained by investigating the physiochemical properties of SEI and the corresponding metallic Li plating behavior.[34,35] Therefore, the solvation state of NO_3^- and the interactions between NO_3^- and other solvents or anions in the solvation sheath are significantly required.

In this contribution, 2.0 M lithium bis(fluorosulfonyl)imide (LiFSI) and 0.20 M lithium nitrate ($LiNO_3$) in dimethoxyethane (DME) were selected as a model system to probe the interactions among various anions. This system was denoted as LiFSI/$LiNO_3$ electrolyte. The effect of the $LiNO_3$ concentration was also investigated. In addition to $LiNO_3$, both lithium perchlorate ($LiClO_4$) and LiFSI were selected rationally to further prove the concept of anion regulation. In this work, it is demonstrated that the introduction of NO_3^- alters the solvation structure of FSI^- in the solvation sheath, thus promoting the decomposition of FSI^- and generating uniform SEI with an abundance of $LiSO_x$, LiF, and LiN_xO_y. Moreover, the key role of NO_3^- is also disclosed from the aspect of the fundamental solvation component and structure. Furthermore, the electrochemical stability window of the electrolyte is widened, and the aluminum (Al) current collector is well protected.

The adequate reduction behavior on an anode and oxidation stability toward a cathode are prerequisites for an electrolyte applied in practical batteries. Both the reduction and oxidation potentials are direct descriptors for screening electrolyte. When there is only FSI^- or NO_3^- in DME, the initial reduction potentials of FSI^- and NO_3^- are at 1.3 and 1.7 V, respectively (Figure 1a). When NO_3^- is mixed with FSI^- in DME, the reduction potential of NO_3^- remains constant. However, the reduction potential of FSI^- is overlapped. The invariability of the reduction potential of NO_3^- contributes to rendering its beneficial role for stable SEI.[36]

DOI: 10.1021/acsenergylett.8b02376
ACS Energy Lett. 2019, 4, 411−416

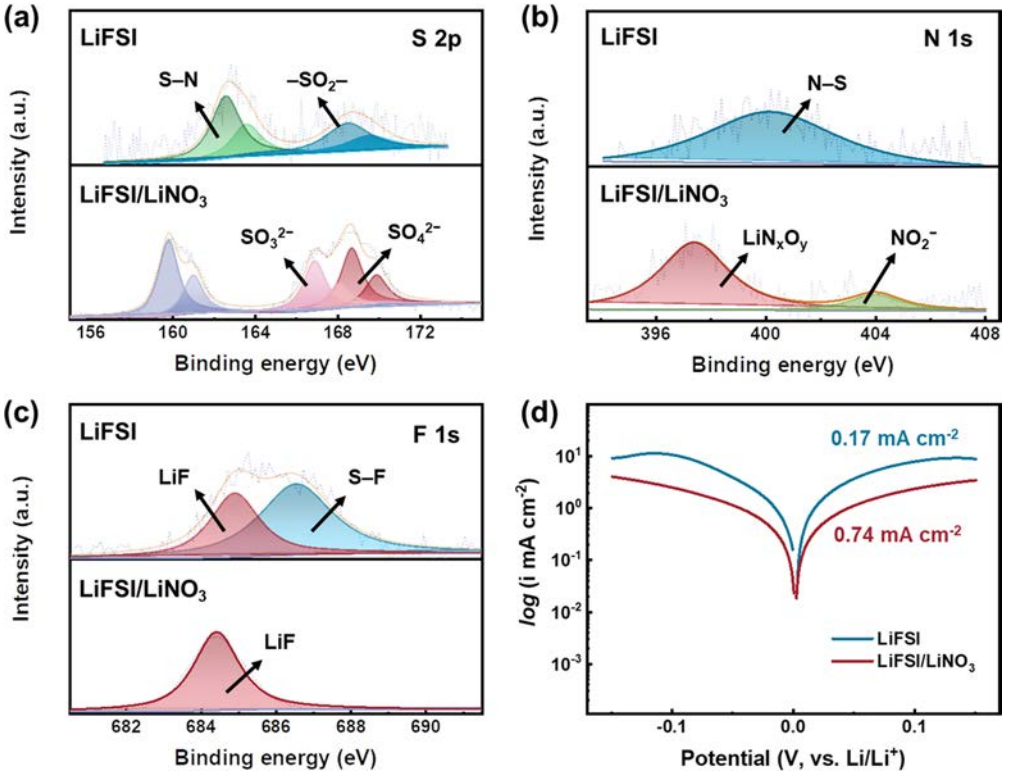

Figure 3. XPS spectra of SEI after etching for 1 min on a Li anode surface after 10 cycles in Li|Li cells with LiFSI or LiFSI/$LiNO_3$ electrolyte. (a) S 2p, (b) N 1s, and (c) F 1s spectra. (d) Tafel plots obtained from a cyclic voltammetry test in Li|Li cells with a scan rate of 1.0 mV s^{-1}.

The oxidation decomposition of LiFSI electrolyte begins at 3.3 V (Figure 1b). Even though the concentration of LiFSI increases to 4.0 M, the oxidation window is only within 3.7 V (Figure S1a). When 0.20 M NO_3^- was added into LiFSI electrolyte, the oxidation tolerance of electrolyte was enlarged to 4.3 V. The enlarged oxidation window was also confirmed by a linear sweep voltammetry test using platinum foil as the working electrode (Figure S1b). The oxidation window of the electrolyte depends on the concentration of $LiNO_3$. With the increase of $LiNO_3$ concentration, the oxidation window of the electrolyte widens from 4.1 to 4.3 V and then remains at 4.3 V (Figure S1c). Therefore, the oxidation stability window of the electrolyte is widened by introducing NO_3^-, rendering the feasibility of employing low concentration LiFSI electrolyte in rechargeable batteries without significantly decreasing the ionic conductivity (Table S1).

The LiFSI/$LiNO_3$ electrolyte was further evaluated in Li|$LiFePO_4$ batteries. The lifespan of a cell with LiFSI electrolyte is only 36 cycles (Figure 2a). However, 500 cycles with 80% capacity retention and stable Coulombic efficiency (CE) were achieved in a cell with LiFSI/$LiNO_3$ electrolyte. The $LiNO_3$ concentration had almost no effect on the cycling performance and CE of Li|$LiFePO_4$ batteries at initial stages (Figure S2a). When 50 μm Li metal was employed to check the performance of various electrolytes, the stability of the LiFSI/$LiNO_3$ electrolyte was also proved (Figure S2b). The stable cycling performance with a higher areal capacity of 2.0 mAh cm^{-2} was still maintained in LiFSI/$LiNO_3$ electrolyte (Figure S3a–c). Excellent rate performance of batteries was also achieved in the LiFSI/$LiNO_3$ electrolyte (Figure S3d). Moreover, the introduction of NO_3^- avoided oxidation decomposition of the electrolyte and corrosion of Al foils (Figure S4), which was a notorious issue when LiFSI is employed as the salt in an electrolyte.[37] The overcharge capacity in LiFSI electrolyte after 40 cycles (Figure 2b) is mainly induced by the decomposition of electrolyte and corrosion of Al foils. According to previous reports, the lifespans of Li|$LiFePO_4$ batteries using carbonate electrolyte at the same test conditions are only 172 cycles.[13] Therefore, the Li anode is well protected in LiFSI/$LiNO_3$ electrolyte during long cycling tests.

The deposition morphology of cycled Li in LiFSI/$LiNO_3$ electrolyte is denser and more uniform than that in LiFSI electrolyte (Figures 2c,d and S5). Therefore, the polarization voltage of the Li|Li cells with NO_3^- is more stable (Figure S6). Interestingly, the morphology of cycled Li obtained in Li|$LiFePO_4$ batteries at the same areal capacity is much different from that in Li|Li cells (Figure S7) despite denser Li in LiFSI/$LiNO_3$ than that in LiFSI electrolyte. The Li plating/stripping in full batteries is more aggressive, in which transition metal ions can dissolve and migrate to the anode, impacting the formation of SEI and the following Li deposition.

The Li deposition behavior is mainly dictated by the uniformity of the SEI on the Li anode. Therefore, in-depth X-ray photoelectron spectroscopy (XPS) was conducted and demonstrated the completed decomposition of FSI^- while introducing NO_3^-. XPS spectra of SEI after etching for 1 min on a Li anode surface are compared (Figure 3). In S 2p spectra, two peaks of S–N (162.1/163.3 eV, for $2p^{3/2}/2p^{1/2}$, hereinafter) and $-SO_2-$ (169.2/170.4 eV) are derived from the original FSI^- (Figure 3a). The preservation of the S–N bond and $-SO_2-$ species indicates the incomplete decomposition of FSI^-. While introducing NO_3^-, three new peaks assigned to Li_2S (159.8/161.0 eV), SO_3^{2-} (166.9/168.1 eV), and SO_4^{2-} (168.7/169.9 eV) emerge. The appearance of species in a lower oxidation state suggests complete decomposition of FSI^-. Similarly, the N–S (400.1 eV) in the LiFSI electrolyte in

DOI: 10.1021/acsenergylett.8b02376
ACS Energy Lett. 2019, 4, 411–416

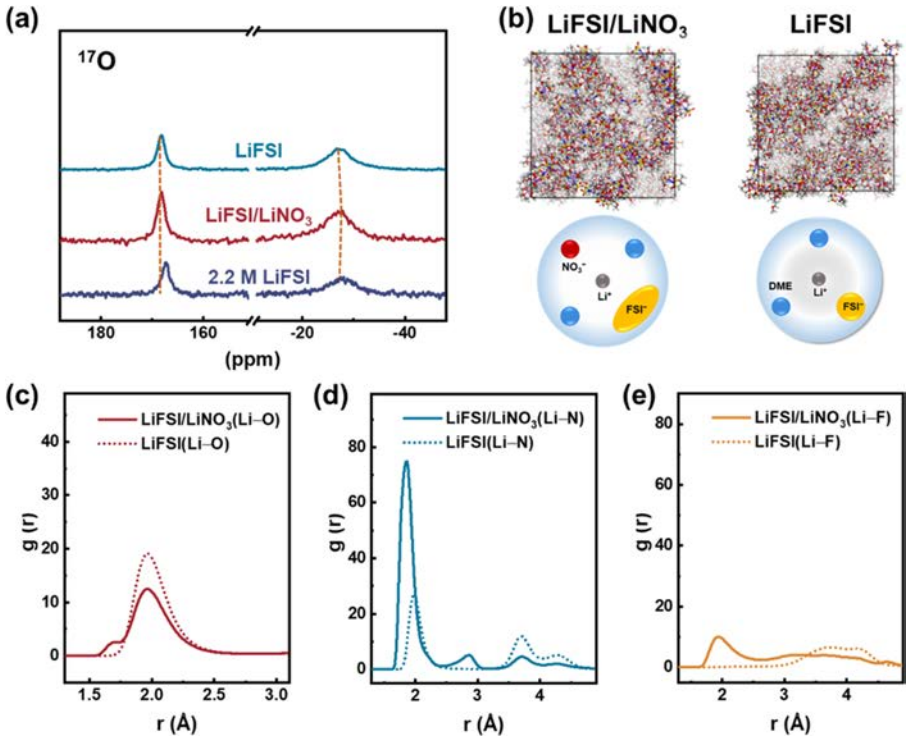

Figure 4. (a) Natural abundance ^{17}O NMR spectra of various electrolytes measured at 50°C. (b) Top panel: snapshots of the MD simulation boxes of LiFSI/LiNO$_3$ and LiFSI electrolyte. Colors for different atoms: H-white, Li-purple, C-gray, O-red, N-blue, F-green, and S-yellow. The unsolvated solvents are in light gray. Bottom panel: schematics of the solvation structure of Li ions in corresponding electrolyte. The magnified snapshots of (b) are shown in Figure S11. MD simulations of (c) Li–O, (d) Li–N, and (e) Li–F radial distribution functions, $g(r)$.

N 1s spectra also confirms the incomplete decomposition. Both LiN_xO_y (397.4 eV) and NO_2^- (404.0 eV) are from the decomposition of $LiNO_3$ (Figure 3b). Moreover, the disappearance of S–F (686.4 eV, Figure 3c) in LiFSI/$LiNO_3$ electrolyte confirms the complete decomposition of FSI^- in the presence of NO_3^-, which leads to more content of LiF (684.8 eV) in SEI. XPS spectra of SEI after etching for 4 min were further investigated to provide more information on the components of SEI at different depths (Figure S8). The species in SEI at different etching times are the same. However, the content of different species changes with increasing depth in both LiFSI and LiFSI/$LiNO_3$ electrolytes. The atomic concentrations of F, S, and N in the SEI obtained in LiFSI/$LiNO_3$ are higher than those in the LiFSI electrolyte (Figure S9). Consequently, complete decomposition of FSI^- is promoted to generate LiF and $LiSO_x$ in the presence of NO_3^-, then contributing to uniform SEI and Li deposition together with LiN_xO_y.

The exchange current density (I_0) was employed to further investigate surface diffusion resistance of SEIs (Figures 3d and S10a).[38] The exchange current density for Li plating/stripping in LiFSI/$LiNO_3$ electrolyte (I_0 = 0.74 mA cm^{-2}) is more than 4 times larger than that in LiFSI electrolyte (I_0 = 0.17 mA cm^{-2}). Hence, the abundance of $LiSO_x$, LiF, and LiN_xO_y also contributes to the low surface barrier of SEIs formed in LiFSI/$LiNO_3$ electrolyte combined with the results of electrochemical impedance spectroscopy (Figure S10b).

The change of components of SEI reflects the variation of the solvation sheath of Li ions. Both ^{17}O nuclear magnetic resonance (NMR) and molecular dynamics (MD) simulations were further performed to probe the detailed changes.[39] The chemical shifts at around 168.0 and −26.0 ppm in LiFSI electrolyte are assigned to the sulfonyl oxygen atoms (O_{FSI^-}) of FSI^- and the ethereal oxygen atoms (O_{DME}) of DME, respectively, which is consistent with previous reports.[40] When 0.20 M NO_3^- or FSI^- is added into 2.0 M LiFSI electrolyte, the peaks of O_{DME} shift upfield (Figure S12). Accordingly, the oxidation window widens with decreasing free solvents (Figures 1b and S1a). Moreover, the addition of NO_3^- enhances the ion–dipole interaction between Li ions and DME solvents more intensively compared with FSI^-, which further widens the oxidation window of electrolyte.

The peak of O_{FSI^-} (167.3 ppm) in 2.2 M LiFSI electrolyte shifts upfield by 0.9 ppm compared with that of 2.0 M LiFSI electrolyte (168.2 ppm, Figures 4a and S12). More FSI^- anions participate in the solvation sheath in 2.2 M LiFSI due to decreased free solvents, leading to a decreased chemical shift. However, when 0.2 M NO_3^- is introduced to 2.0 M LiFSI electrolyte, the peak of O_{FSI^-} (168.0 ppm) only shifts upfield by 0.2 ppm. Under the same FSI^-/DME ratio in LiFSI/$LiNO_3$ electrolyte, a higher Li^+/FSI^- ratio induces a smaller shift of the O_{FSI^-} peak compared with LiFSI electrolyte, indicating that NO_3^- is involved in solvation instead of more FSI^- anions.

According to the radial distribution functions generated from a 2.0 ns MD simulations in the canonical ensemble (*NVT*) at 298 K, the solvation structure of FSI^- anions highly depends on the presence of NO_3^- (Figure 4b–e). The new peaks of Li–O (1.7 Å, Figure 4c) and Li–N (2.9 Å, Figure 4d) prove the participation of NO_3^- in the solvation sheath in LiFSI/$LiNO_3$ electrolyte. The increase of Li–N at around 2.0 Å and the decrease of Li–O at around 2.0 Å indicate that more FSI^- interacts with Li ions through the Li–N bond rather than the Li–O bond in LiFSI/$LiNO_3$ electrolyte. Especially, the emerging Li–F peak at around 2.0 Å exhibits that the F atom

DOI: 10.1021/acsenergylett.8b02376
ACS Energy Lett. 2019, 4, 411–416

in FSI^- can interact with Li ions directly. Therefore, the introduction of NO_3^- regulates the interactions between Li ions and FSI^- and results in polarization of FSI^-. Polarized FSI^- is activated and thus decomposes completely (Figure S13), which combines with NO_3^- to generate favorable SEI with an abundance of $LiSO_x$, LiF, and LiN_xO_y.

On the basis of the above insights and understandings, LiFSI/$LiClO_4$ electrolyte was designed. When 0.20 M $LiClO_4$ was added into LiFSI electrolyte, the oxidation stable window of the electrolyte was widened to 4.4 V (Figure S14a). When it was applied to working batteries, LiFSI/$LiClO_4$ electrolyte exhibited a stable and long cycling life compared to LiFSI electrolyte (Figure S14b,c). When 0.20 M ClO_4^- was added into 2.0 M LiFSI electrolyte, the peaks of O_{DME} shifted upfield by 1.4 ppm (Figure S15a), which is larger than that induced by the addition of 0.20 M $LiNO_3$ (1.1 ppm). Accordingly, the oxidation window of LiFSI/$LiClO_4$ is larger than that of LiFSI/$LiNO_3$ (Figure S15b). Therefore, the addition of ClO_4^- further enhances the ion−dipole interaction between Li ions and DME solvents compared with the addition of NO_3^-. The peak of O_{FSI^-} (167.0 ppm) in LiFSI/$LiClO_4$ electrolyte shifts upfield by 1.2 ppm compared with 2.0 M LiFSI electrolyte (Figure S15a). The decreased chemical shift of O_{FSI^-} is induced by participation of ClO_4^- in the solvation sheath, which is similar to the results of NO_3^-. However, the decreased chemical shift of O_{FSI^-} in LiFSI/$LiClO_4$ and LiFSI/$LiNO_3$ is 1.2 and 0.2 ppm, respectively, illustrating that the effect of different anions on the polarization of FSI^- is distinctive. The successful design of LiFSI/$LiClO_4$ electrolyte confirms the generality of the interactions among anions and the effectiveness of regulating anions in the solvation sheath for electrolyte innovation.

In conclusion, stable Li metal full batteries and stable CEs were achieved by a new and general strategy, regulating the anions in the solvation sheath. The effect of anion regulation on the components and structure of the solvation sheath was jointly disclosed by ^{17}O NMR spectra and MD simulations. The solvation structure of FSI^- is mediated and polarized by other anions, such as NO_3^-, which induces complete decomposition of FSI^-. Therefore, a uniform and less resistive SEI is achieved with an abundance of $LiSO_x$, LiF, and LiN_xO_y. Moreover, the oxidation stability window is widened to 4.3 V, and corrosion of the Al current collector is avoided. The generality of the above understanding and strategy is also verified by the design of LiFSI/$LiClO_4$ electrolyte. This work affords profound insight into understanding the interactions among various anions on regulating the solvation sheath of Li ions in electrolytes for rechargeable batteries, which can be extended into other battery chemistry, such as sodium batteries. This work also inspires new adventures in designing electrolytes by simple anion regulation in the solvation sheath for high-energy-density and safe Li batteries and other types of batteries.

■ ASSOCIATED CONTENT

Supporting Information

The Supporting Information is available free of charge on the ACS Publications website at DOI: 10.1021/acsenergylett.8b02376.

Experimental procedures, MD simulation details, linear sweep voltammetry curves, battery cycling performance, electrochemical performance, magnified morphologies of Li, voltage−time curves of LilLi cells, XPS spectra of the SEI, atomic concentrations, Tafel plots, natural abundance spectra, chemical structure of FSI^-, conductivity data, and water content data (PDF)

■ AUTHOR INFORMATION

Corresponding Author

*E-mail: zhang-qiang@mails.tsinghua.edu.cn.

ORCID

Xue-Qiang Zhang: 0000-0003-2856-1881
Xiang Chen: 0000-0002-7686-6308
Bo-Quan Li: 0000-0002-9544-5795
Jia-Qi Huang: 0000-0001-7394-9186
Qiang Zhang: 0000-0002-3929-1541

Author Contributions

X.-Q.Z. and X.C. contributed equally to this work.

Notes

The authors declare no competing financial interest.

■ ACKNOWLEDGMENTS

This work was supported by the National Key Research and Development Program (2016YFA0202500 and 2016YFA0200102) and the National Natural Science Foundation of China (21676160, 21825501, 21808121, and 21805161). The authors acknowledge support from Tsinghua National Laboratory for Information Science and Technology for theoretical simulations.

■ REFERENCES

(1) Tarascon, J. M.; Armand, M. Issues and Challenges Facing Rechargeable Lithium Batteries. *Nature* **2001**, *414*, 359−367.
(2) Cheng, X. B.; Zhang, R.; Zhao, C. Z.; Zhang, Q. Toward Safe Lithium Metal Anode in Rechargeable Batteries: A Review. *Chem. Rev.* **2017**, *117*, 10403−10473.
(3) Lin, D.; Liu, Y.; Cui, Y. Reviving the Lithium Metal Anode for High-Energy Batteries. *Nat. Nanotechnol.* **2017**, *12*, 194−206.
(4) Zhang, X. Q.; Zhao, C. Z.; Huang, J. Q.; Zhang, Q. Recent Advances in Energy Chemical Engineering of Next-Generation Lithium Batteries. *Engineering* **2018**, *4*, 831−847.
(5) Tikekar, M. D.; Choudhury, S.; Tu, Z. Y.; Archer, L. A. Design Principles for Electrolytes and Interfaces for Stable Lithium-Metal Batteries. *Nat. Energy* **2016**, *1*, 16114.
(6) Li, Y.; Li, Y.; Pei, A.; Yan, K.; Sun, Y.; Wu, C. L.; Joubert, L. M.; Chin, R.; Koh, A. L.; Yu, Y.; et al. Atomic Structure of Sensitive Battery Materials and Interfaces Revealed by Cryo-Electron Microscopy. *Science* **2017**, *358*, 506−510.
(7) Li, Y.; Huang, W.; Li, Y.; Pei, A.; Boyle, D. T.; Cui, Y. Correlating Structure and Function of Battery Interphases at Atomic Resolution Using Cryoelectron Microscopy. *Joule* **2018**, *2*, 2167−2177.
(8) Goodenough, J. B.; Kim, Y. Challenges for Rechargeable Li Batteries. *Chem. Mater.* **2010**, *22*, 587−603.
(9) Aurbach, D. Review of Selected Electrode−Solution Interactions Which Determine the Performance of Li and Li Ion Batteries. *J. Power Sources* **2000**, *89*, 206−218.
(10) Xu, K. Electrolytes and Interphases in Li-Ion Batteries and Beyond. *Chem. Rev.* **2014**, *114*, 11503−11618.
(11) Abe, T.; Fukuda, H.; Iriyama, Y.; Ogumi, Z. Solvated Li-Ion Transfer at Interface between Graphite and Electrolyte. *J. Electrochem. Soc.* **2004**, *151*, A1120−A1123.
(12) Xu, K.; Lam, Y.; Zhang, S. S.; Jow, T. R.; Curtis, T. B. Solvation Sheath of Li^+ in Nonaqueous Electrolytes and Its Implication of Graphite/Electrolyte Interface Chemistry. *J. Phys. Chem. C* **2007**, *111*, 7411−7421.

DOI: 10.1021/acsenergylett.8b02376
ACS Energy Lett. 2019, 4, 411−416

(13) Zhang, X. Q.; Chen, X.; Cheng, X. B.; Li, B. Q.; Shen, X.; Yan, C.; Huang, J. Q.; Zhang, Q. Highly Stable Lithium Metal Batteries Enabled by Regulating the Solvation of Lithium Ions in Nonaqueous Electrolytes. *Angew. Chem., Int. Ed.* **2018**, *57*, 5301−5305.
(14) Markevich, E.; Salitra, G.; Chesneau, F.; Schmidt, M.; Aurbach, D. Very Stable Lithium Metal Stripping-Plating at a High Rate and High Areal Capacity in Fluoroethylene Carbonate-Based Organic Electrolyte Solution. *ACS Energy Lett.* **2017**, *2*, 1321−1326.
(15) Chen, X.; Shen, X.; Li, B.; Peng, H. J.; Cheng, X. B.; Li, B. Q.; Zhang, X. Q.; Huang, J. Q.; Zhang, Q. Ion−Solvent Complexes Promote Gas Evolution from Electrolytes on a Sodium Metal Anode. *Angew. Chem., Int. Ed.* **2018**, *57*, 734−737.
(16) Su, C. C.; He, M.; Amine, R.; Chen, Z.; Amine, K. The Relationship between the Relative Solvating Power of Electrolytes and Shuttling Effect of Lithium Polysulfides in Lithium−Sulfur Batteries. *Angew. Chem., Int. Ed.* **2018**, *57*, 12033−12036.
(17) Chen, X.; Li, H. R.; Shen, X.; Zhang, Q. The Origin of the Reduced Reductive Stability of Ion−Solvent Complexes on Alkali and Alkaline Earth Metal Anodes. *Angew. Chem., Int. Ed.* **2018**, *57*, 16643−16647.
(18) von Wald Cresce, A.; Gobet, M.; Borodin, O.; Peng, J.; Russell, S. M.; Wikner, E.; Fu, A.; Hu, L.; Lee, H. S.; Zhang, Z.; et al. Anion Solvation in Carbonate-Based Electrolytes. *J. Phys. Chem. C* **2015**, *119*, 27255−27264.
(19) Ming, J.; Cao, Z.; Wahyudi, W.; Li, M.; Kumar, P.; Wu, Y.; Hwang, J. Y.; Hedhili, M. N.; Cavallo, L.; Sun, Y. K.; et al. New Insights on Graphite Anode Stability in Rechargeable Batteries: Li Ion Coordination Structures Prevail over Solid Electrolyte Interphases. *ACS Energy Lett.* **2018**, *3*, 335−340.
(20) Zheng, J.; Engelhard, M. H.; Mei, D.; Jiao, S.; Polzin, B. J.; Zhang, J. G.; Xu, W. Electrolyte Additive Enabled Fast Charging and Stable Cycling Lithium Metal Batteries. *Nat. Energy* **2017**, *2*, 17012.
(21) Zhang, S. S. A Review on Electrolyte Additives for Lithium-Ion Batteries. *J. Power Sources* **2006**, *162*, 1379−1394.
(22) Fan, X.; Chen, L.; Borodin, O.; Ji, X.; Chen, J.; Hou, S.; Deng, T.; Zheng, J.; Yang, C.; Liou, S. C.; et al. Non-Flammable Electrolyte Enables Li-Metal Batteries with Aggressive Cathode Chemistries. *Nat. Nanotechnol.* **2018**, *13*, 715−722.
(23) Park, S. J.; Hwang, J. Y.; Yoon, C. S.; Jung, H. G.; Sun, Y. K. Stabilization of Lithium-Metal Batteries Based on the in-situ Formation of a Stable Solid Electrolyte Interphase Layer. *ACS Appl. Mater. Interfaces* **2018**, *10*, 17985−17993.
(24) von Wald Cresce, A.; Borodin, O.; Xu, K. Correlating Li^+ Solvation Sheath Structure with Interphasial Chemistry on Graphite. *J. Phys. Chem. C* **2012**, *116*, 26111−26117.
(25) Yamada, Y.; Furukawa, K.; Sodeyama, K.; Kikuchi, K.; Yaegashi, M.; Tateyama, Y.; Yamada, A. Unusual Stability of Acetonitrile-Based Superconcentrated Electrolytes for Fast-Charging Lithium-Ion Batteries. *J. Am. Chem. Soc.* **2014**, *136*, 5039−5046.
(26) Qian, J.; Henderson, W. A.; Xu, W.; Bhattacharya, P.; Engelhard, M.; Borodin, O.; Zhang, J. G. High Rate and Stable Cycling of Lithium Metal Anode. *Nat. Commun.* **2015**, *6*, 6362.
(27) Ueno, K.; Yoshida, K.; Tsuchiya, M.; Tachikawa, N.; Dokko, K.; Watanabe, M. Glyme−Lithium Salt Equimolar Molten Mixtures: Concentrated Solutions or Solvate Ionic Liquids? *J. Phys. Chem. B* **2012**, *116*, 11323−11331.
(28) Suo, L.; Borodin, O.; Gao, T.; Olguin, M.; Ho, J.; Fan, X.; Luo, C.; Wang, C. S.; Xu, K. "Water-in-Salt" Electrolyte Enables High-Voltage Aqueous Lithium-Ion Chemistries. *Science* **2015**, *350*, 938−943.
(29) Suo, L.; Xue, W.; Gobet, M.; Greenbaum, S. G.; Wang, C.; Chen, Y.; Yang, W.; Li, Y.; Li, J. Fluorine-Donating Electrolytes Enable Highly Reversible 5-V-Class Li Metal Batteries. *Proc. Natl. Acad. Sci. U. S. A.* **2018**, *115*, 1156−1161.
(30) Fan, X. L.; Chen, L.; Ji, X.; Deng, T.; Hou, S. Y.; Chen, J.; Zheng, J.; Wang, F.; Jiang, J. J.; Xu, K.; et al. Highly Fluorinated Interphases Enable High-Voltage Li-Metal Batteries. *Chem* **2018**, *4*, 174−185.
(31) Aurbach, D.; Pollak, E.; Elazari, R.; Salitra, G.; Kelley, C. S.; Affinito, J. On the Surface Chemical Aspects of Very High Energy Density, Rechargeable Li−Sulfur Batteries. *J. Electrochem. Soc.* **2009**, *156*, A694−A702.
(32) Iliksu, M.; Khetan, A.; Yang, S.; Simon, U.; Pitsch, H.; Sauer, D. U. Elucidation and Comparison of the Effect of LiTFSi and $LiNO_3$ Salts on Discharge Chemistry in Nonaqueous Li−O_2 Batteries. *ACS Appl. Mater. Interfaces* **2017**, *9*, 19319−19325.
(33) Yan, C.; Yao, Y. X.; Chen, X.; Cheng, X. B.; Zhang, X. Q.; Huang, J. Q.; Zhang, Q. Lithium Nitrate Solvation Chemistry in Carbonate Electrolyte Sustains High-Voltage Lithium Metal Batteries. *Angew. Chem., Int. Ed.* **2018**, *57*, 14055−14059.
(34) Xiong, S.; Xie, K.; Diao, Y.; Hong, X. Properties of Surface Film on Lithium Anode with $LiNO_3$ as Lithium Salt in Electrolyte Solution for Lithium−Sulfur Batteries. *Electrochim. Acta* **2012**, *83*, 78−86.
(35) Li, W.; Yao, H.; Yan, K.; Zheng, G.; Liang, Z.; Chiang, Y. M.; Cui, Y. The Synergetic Effect of Lithium Polysulfide and Lithium Nitrate to Prevent Lithium Dendrite Growth. *Nat. Commun.* **2015**, *6*, 7436.
(36) Xiong, S.; Xie, K.; Diao, Y.; Hong, X. Characterization of the Solid Electrolyte Interphase on Lithium Anode for Preventing the Shuttle Mechanism in Lithium−Sulfur Batteries. *J. Power Sources* **2014**, *246*, 840−845.
(37) Abouimrane, A.; Ding, J.; Davidson, I. J. Liquid Electrolyte Based on Lithium Bis-Fluorosulfonyl Imide Salt: Aluminum Corrosion Studies and Lithium Ion Battery Investigations. *J. Power Sources* **2009**, *189*, 693−696.
(38) Zhao, Q.; Tu, Z.; Wei, S.; Zhang, K.; Choudhury, S.; Liu, X.; Archer, L. A. Building Organic/Inorganic Hybrid Interphases for Fast Interfacial Transport in Rechargeable Metal Batteries. *Angew. Chem., Int. Ed.* **2018**, *57*, 992−996.
(39) Bogle, X.; Vazquez, R.; Greenbaum, S.; Cresce, A. V. W.; Xu, K. Understanding Li^+−Solvent Interaction in Nonaqueous Carbonate Electrolytes with ^{17}O NMR. *J. Phys. Chem. Lett.* **2013**, *4*, 1664−1668.
(40) Wan, C.; Hu, M. Y.; Borodin, O.; Qian, J.; Qin, Z.; Zhang, J. G.; Hu, J. Z. Natural Abundance ^{17}O, ^{6}Li NMR and Molecular Modeling Studies of the Solvation Structures of Lithium Bis(Fluorosulfonyl)-Imide/1,2-Dimethoxyethane Liquid Electrolytes. *J. Power Sources* **2016**, *307*, 231−243.

DOI: 10.1021/acsenergylett.8b02376
ACS Energy Lett. 2019, 4, 411−416